HEFAT2014
10th International Conference on Heat Transfer, Fluid Mechanics and Thermodynamics
14 – 16 July 2014
Orlando, Florida

HEAT TRANSFER CHARACTERISTICS OF JET IMPINGEMENT ONTO A HEATED DISC BOUNDED BY A CYLINDRICAL WALL

Nasif G.,* Barron R.M. and Balachandar R.
*Author for correspondence
Department of Mechanical, Automotive &Material Engineering
University of Windsor
Windsor, Ontario
Canada
E-mail: nasifg@uwindsor.ca

ABSTRACT

A numerical investigation to determine the thermal characteristics of an unsubmerged axisymmetric oil jet impinging in a confined space on both stationary and high speed reciprocated moving discs with uniform heat flux has been undertaken. The volume of fluid (VOF) method utilizing a high resolution interface capturing (HRIC) scheme was used to perform the two-phase (air-liquid) simulations. The governing 3D Navier-Stokes equations and energy equation were solved using a finite volume discretization. The conjugate heat transfer (CHT) method was used to obtain a coupled heat transfer solution between the solid and fluid, yielding a more accurate prediction for the heat transfer coefficient. A piston motion equation is used to provide a reciprocating motion for the disc inside a confined cylindrical space.

NOMENCLATURE

B	$2(d/u_f)(\partial u_r/\partial r)_{r\to 0}$
d	Nozzle diameter (mm)
DBP	Dead Bottom Position
DTP	Dead Top Position
H	Nozzle-to-disc spacing (mm)
h	Heat transfer coefficient (W/m^{2}K)
k	Thermal conductivity of oil (W/m^{2}K)
Nu	Nusselt number = hd/k_{oil} (dimensionless)
Nu_o	Stagnation zone Nusselt number (dimensionless)
Pr	Prandtl number (dimensionless)
Re_d	Reynolds number of the jet = $u_f d/\nu$
r	Radius measured from point of jet impact (mm)
T	Temperature (°C)
u_f	Bulk velocity at the nozzle exit (m/s)
$u_{f,relative}$	Relative velocity between disc and jet (m/s)
u_r	Radial velocity just above viscous layer (m/s)
ν	Kinematic viscosity (m^2/s)
Θ	Crank angle of the rotating machine (deg.)

INTRODUCTION

When an axisymmetric jet strikes a fixed surface, the flow field can be divided into an outer inviscid region and an inner viscous boundary layer. A thin stagnation zone forms perpendicular to the impingement axis as shown in Figure 1. This layer, in which the convective heat transfer coefficient can reach tens of kW/m^{2}K, exhibits little resistance to heat flow. After impingement on the surface, the flow travels radially and spreads thinner, causing the thickness of the liquid film adjacent to the wall to decrease with radius. At a short distance (r_1), the outer edge of the boundary layer will come into contact with the surface of the fluid film. At this point, the fluid film thickness begins to increase at larger radii due to the viscous drag, slowing flow down and thickening the liquid layer.

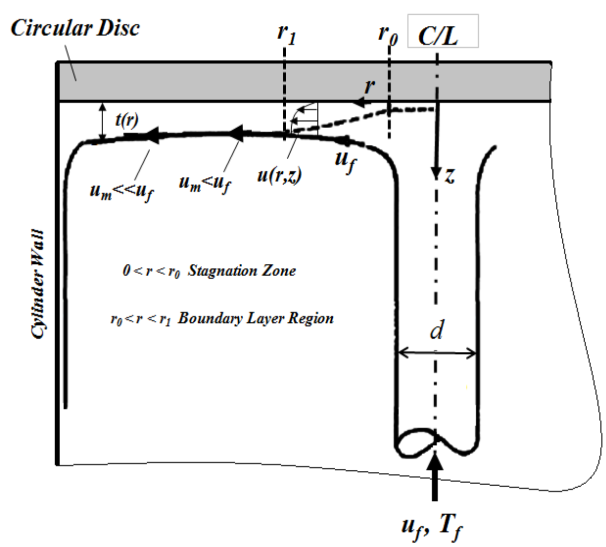

Figure 1 Jet and film flow showing hydrodynamic evolution

Both experimental [1-5] and numerical [6-9] techniques have been used to study heat transfer characteristics of impinging jets. However, there are still other important issues to be addressed, such as jet impingement heat transfer onto a high speed reciprocated moving boundary, higher nozzle-to-target spacing, and higher impingement surface temperature or heat flux. These parameters are crucial in providing better insight into various industrial applications. For example, automotive engine performance can be improved by increasing the conversion of chemical energy in the fuel into kinetic energy. However, this may lead to excessively high temperature in the pistons, which can cause a number of problems. A jet of oil impinging onto the piston surface can be used to prevent overheating of the pistons.

A numerical study to investigate the thermal characteristics of impinging jet onto a fixed disc placed in a confined cylindrical space and subjected to uniform heat flux on the surface was carried out in [10], using different nozzle diameters and flow conditions. The research revealed that the normalized local Nusselt number had a distinct dependence on the radial location and only a slight dependence on the Reynolds number. The extent of the stagnation region on the disc was found to be variable and not constant as suggested by many experimental studies; it is a function of the radial velocity gradient at the stagnation point. The effect of the extent of the stagnation zone on the Nusselt number is small for larger nozzles. However, for smaller diameters, the difference in predicted stagnation zone Nusselt number can be as much as 22%. For a given Reynolds number, the temperature distribution on the fluid-solid interface was found to be more uniform for larger nozzles compared to smaller ones. Smaller nozzles provide more efficient spot cooling at the stagnation region and subsequently lower temperature. Expressions for the local and stagnation zone Nusselt number are given in [10]. The correlation for stagnation zone Nusselt number is:

$$Nu_o = 0.0142\, Re_d^{\,0.565} Pr^{0.4} B^{3.41} \qquad (1)$$

Equation (1) predicts the computational data with an average error less than 10%, for all nozzle sizes and jet Reynolds numbers which have been investigated in the study. The spacing term H/d does not appear in the above equation, because this equation is used to predict the stagnation zone Nusselt numbers for long jets, i.e., $H/d > 5$, where nozzle-to-target spacing is insignificant [11]. A numerical investigation to evaluate the effect of nozzle geometry on thermal characteristics for long jet impingement has been undertaken in [12]. The investigation showed that the effect of nozzle geometry is insignificant on thermal characteristics. The viscosity tends to normalize the jet velocity profile in the radial directions for long jets after some distance from the nozzle exit, which results in a constant velocity gradient at the stagnation point.

Experiments were performed in [13] to study the characteristics of an impinging turbulent jet onto a fixed surface subjected to constant heat flux, using different nozzle diameters and a wide range of Reynolds number. The investigations showed an obvious dependence of the stagnation zone Nusselt number on Reynolds number, Prandtl number and velocity gradient and less dependency on nozzle-to-plate spacing. The stagnation point velocity gradient is nozzle diameter dependent and is a linear function of u_f/d in laminar jets. The drawback of using u_f/d as a correlating parameter is its dimensional nature, and there is no obvious reference time scale for use in its normalization. If u_f/d is employed as a correlating parameter with other dimensionless parameters (Nu, Re_d, Pr, H/d), the empirical relation for stagnation zone Nusselt number is given in [13] as:

$$Nu_o = 2.67\, Re_d^{\,0.567} Pr^{0.4} (H/d)^{-0.0336} (u_f/d)^{-0.237} \qquad (2)$$

Equation (2) is considered to be valid for $4000 < Re_d < 52000$ and predicts the experimental data with an average error of 5% and maximum error of 14%, for all nozzles sizes used in the experiments.

The objective of the present study is to numerically investigate the jet impingement thermal characteristics when an axisymmetric, engine oil jet impinges orthogonally onto fixed and moving circular discs subjected to uniform heat flux and bounded by a cylindrical wall. For the moving boundary, a piston motion equation is used to describe a reciprocating motion for the circular disc in the range between 20 to 100 mm away from a 1.0 mm nozzle. Two angular velocities were chosen, i.e., 210 and 630 rad/s, so that the relative velocity between the jet and disc is between 20 to 39 m/s approximately during the cycle with the angular velocity 210 rad/s, and between 3 to 56 m/s approximately during the cycle with the angular velocity 630 rad/s.

COMPUTATIONAL APPROACH

Finite volume based computations using CD-adapco's STAR-CCM+ code with polyhedral cells are performed in the current study. The major advantage of polyhedral cells is that they generally have many neighbours (typically of order 10), so gradients can be much better approximated using linear shape functions. Along the wall and at corners, a polyhedral cell is likely to have at least a couple of neighbours, which allows for a reasonable prediction of both gradients and local flow distribution. The fact that more neighbours means more storage and computing operations per cell is compensated for by a higher accuracy. The k-ω SST model, which is a two-equation eddy-viscosity model, is used as the turbulence model in the present study. Since the flow field involves two different immiscible fluids (oil jet in air), a numerical model to handle two-phase flow is required. Volume of fluid (VOF) is a simplified and efficient method which is capable of capturing the movement of the interface between the mixture phases. High Resolution Interface Capturing (HRIC) [14] is the most common scheme used for interface capturing with the VOF model. The interaction between the heat conduction inside the solid and the flow of fluid along the solid surface, commonly referred to as a conjugate heat transfer process (CHT), is simulated in the current study. Accounting for conjugate heat transfer is particularly important when there are large thermal gradients on the surface or within the solid.

MODEL SETUP

The present transient simulation is used to predict steady state thermal characteristics when an axisymmetric oil jet with temperature at 130°C impinges onto a 10 mm thick aluminum disc placed in a cylindrical confined space. It is worthwhile to mention that although the simulation is transient, we have used the term 'steady state' to describe the final temperature distribution in the disc, because the time scale of the heat transfer from the disc is very large compared with the time scale of the problem itself (i.e., cycle duration) and thus the temperature distribution will not change significantly over the cycle. The simulations were implemented with and without disc motion, i.e., for both a moving and stationary disc. The computational domain and relevant boundary conditions used in this simulation are shown in Figure 2. A 1.0 mm diameter pipe nozzle has been used to produce a fully developed turbulent pipe flow profile, which has been mapped as an inlet boundary condition to the computational domain. The Reynolds number of the jet lies in the turbulent regime (i.e., $Re_d \approx 3000$). The cells were clustered along the jet trajectory, with minimum cell size of 0.075 mm, to prevent the smearing associated with numerical diffusion and preserve the sharpness of the oil-air interface. Fine prism cells were employed adjacent to the disc to resolve the thin film and reduce the artificial dissipation of the oil at these locations. A grid sensitivity study to determine an optimum cell size has been carried out for a stationary boundary [10]. The final cell number chosen for subsequent simulations was based on negligible changes in the stagnation zone Nusselt number and the average disc temperature.

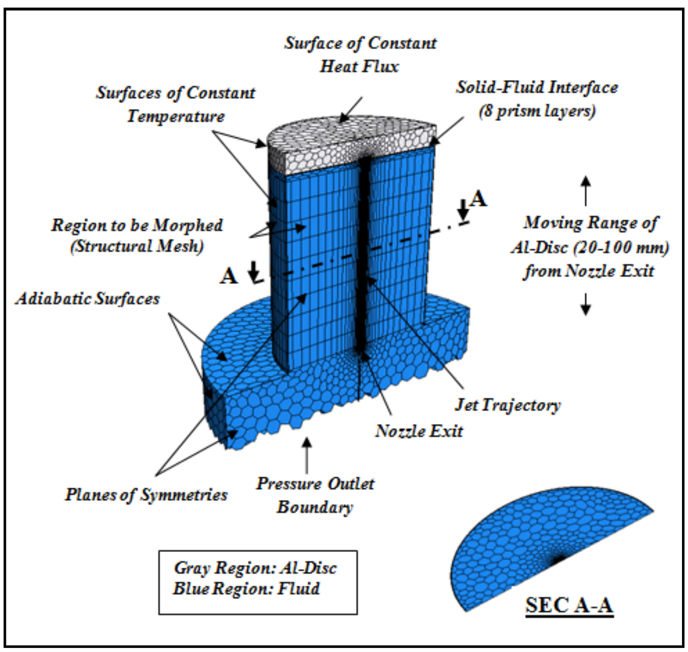

Figure 2 Computational domain and boundary conditions

A one-half segment of the entire geometry was used as a computational domain to reduce the CPU calculation time. Therefore, a symmetry boundary condition is assumed on the central plane of the domain. The top surface of the 90 mm diameter disc is subjected to a uniform heat flux of $q'' = 50$ kW/m^2 [6], while the cylinder and solid disc outer surfaces are kept at constant temperature of T = 130°C. All fluid and air properties, such as dynamic viscosity, density, thermal conductivity and specific heat, are evaluated as a function of the local temperature in the computational domain. The nozzle exit temperature (T = 130°C) is used as the reference temperature for the evaluation of the heat transfer coefficient and Nusselt number.

Validation Process

The numerical predictions of local and stagnation zone Nusselt numbers are validated for a stationary boundary. The validation process given in [10] was employed using three nozzle sizes, over a wide range of Reynolds number. The empirical correlations given in [11] to predict the local and stagnation zone Nusselt number are used for comparison, revealing an average differences in stagnation zone Nusselt number of 3.5, 5.0 and 8.0% corresponding to nozzles sizes of d = 1.0, 2.0 and 4.0 mm, respectively.

RESULTS

In the current simulation, the fluid-solid interface is split into nine consecutive regions for comparison purposes of heat transfer coefficient and temperature, as shown in Figure 3. Region-1 represents approximately the stagnation zone, where the maximum heat transfer coefficient occurs due to the jet impingement. In the following subsections the jet impingement onto both stationary and moving boundaries will be discussed.

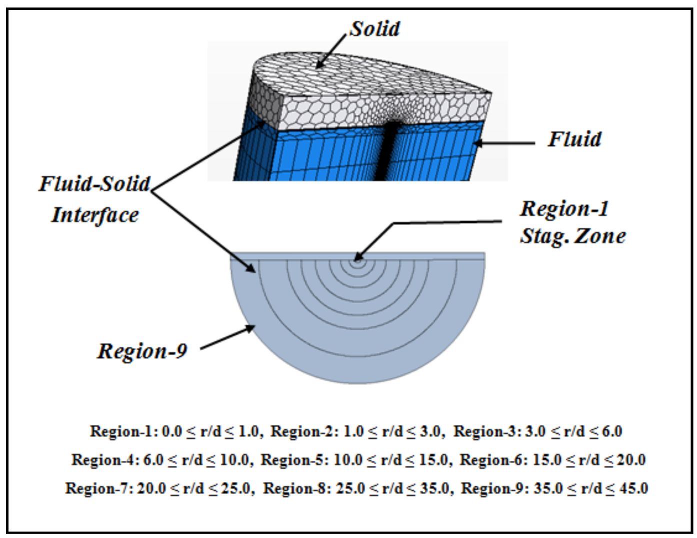

Figure 3 Annular regions at the fluid-solid interface

Jet Impingement onto a Stationary Boundary

Two steady-state simulations were run in the current study, with the disc fixed at its bottom and top positions, 20 and 100 mm away from the nozzle exit, respectively. In these cases, the relative velocity is purely the jet velocity. The temperature profiles in the disc are shown in Figure 4.

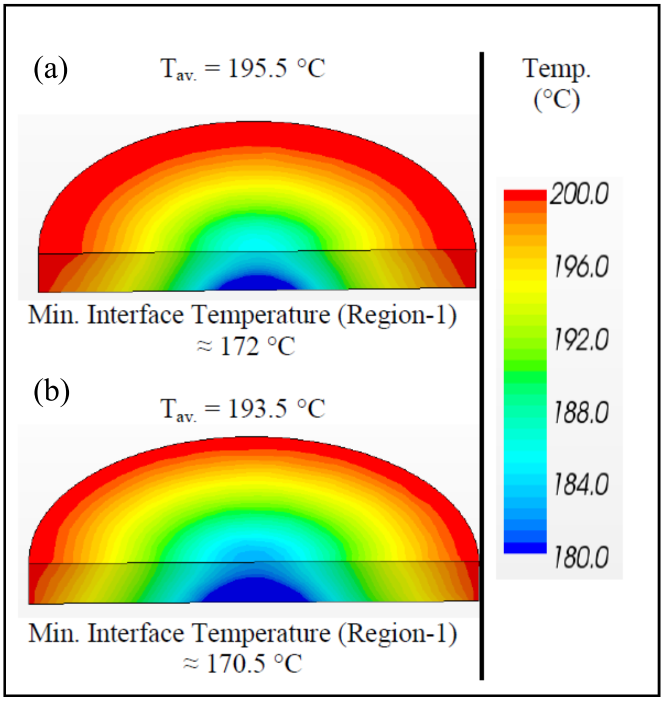

Figure 4 Steady state temperature profiles for stationary disc with cooling jet, at two elevations from the nozzle exit: (a) 20 mm, (b) 100 mm

(a)

Region No.	*Nu*	*HTC ($W/m^2.K$)*
Region-1	151.0	20204
Region-2	109.5	14651
Region-3	77.0	10303
Region-4	48.0	6422
Total Surface Av.	**8.0**	**1070**

(b)

Region No.	*Nu*	*HTC ($W/m^2.K$)*
Region-1	140.0	18732
Region-2	106.0	14183
Region-3	76.0	10169
Region-4	48.0	6422
Total Surface Av.	**10.5**	**1405**

Table 1 Surface average Nusselt number at solid-fluid interface, at two elevations from the nozzle exit: (a) 20 mm, (b) 100 mm

The average heat transfer coefficients (HTC) and corresponding Nusselt numbers on the surface are given in Table 1, for regions 1 - 4. Important observations can be drawn from Figure 4 and Table 1. First, the maximum Nusselt number and minimum temperature occur at the center of the disc. Second, although there is little difference in HTCs at the four consecutive regions in either case, the overall surface average HTC at the interface is higher with the longer jet. Consequently, the volume average temperature and stagnation zone temperature are less for the longer jet.

Figure 5 shows the comparison of the radial velocity and VOF distribution for the two nozzle-to-disc distances. The magnitude of the radial velocity is very similar up to region 4 in both cases, contributing to the similar values of HTC. Beyond region 4, the velocity is higher in the case of the longer jet. Furthermore, the VOF contours indicate that there are differences in the VOF distribution in the two cases. It appears that the dynamics of the interaction is different in the shorter jet, with more splattering (enhanced mist) occurring. The persistent contact of liquid with the disc and increased radial momentum of the flow provides for additional opportunities to enhance the HTC values in the longer jet.

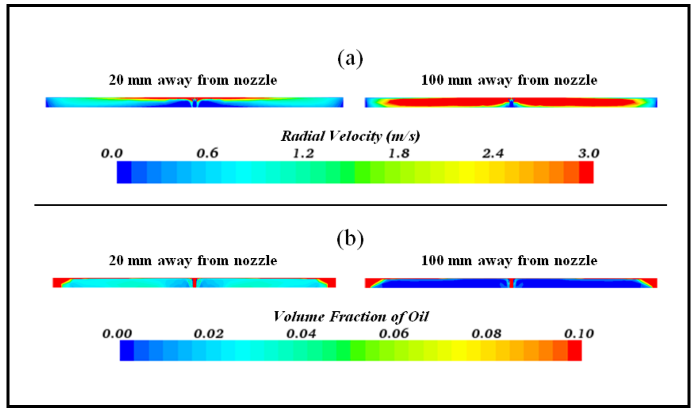

Figure 5 Comparison of radial velocity and VOF distribution for two nozzle-to-disc distances: (a) radial velocity contours, (b) VOF contours

Jet Impingement onto a Moving Boundary

Transient simulations were carried out using two angular velocities to provide the reciprocating motion to the disc. The optimum time steps to prevent jet smearing were found to be 1.0E-6 and 3.3E-6 s corresponding to angular velocities of 210 and 630 rad/s, respectively. The physical time required for each cycle was 0.03 and 0.01 s, corresponding to angular velocities 210 and 630 rad/s, respectively. In terms of CPU time, this requires about 3000 hours to complete the simulation of one cycle (360°).

The Nusselt number behaviour is periodic when the temperature profile in the disc reaches its steady state, as shown in Figure 6. It is obvious from this figure that the maximum relative velocity between the disc and the jet occurs ahead of the maximum heat transfer coefficient or Nusselt number. The phase shift for both angular velocities is approximately 3.0°. After impingement, the flow turns and enters a wall jet region where the flow moves laterally outward parallel to the wall. This lateral flow at the stagnation zone is responsible for the maximum HTC. The turning process will lag the occurrence of the maximum HTC by a few degrees, i.e., 3.0° in the current study.

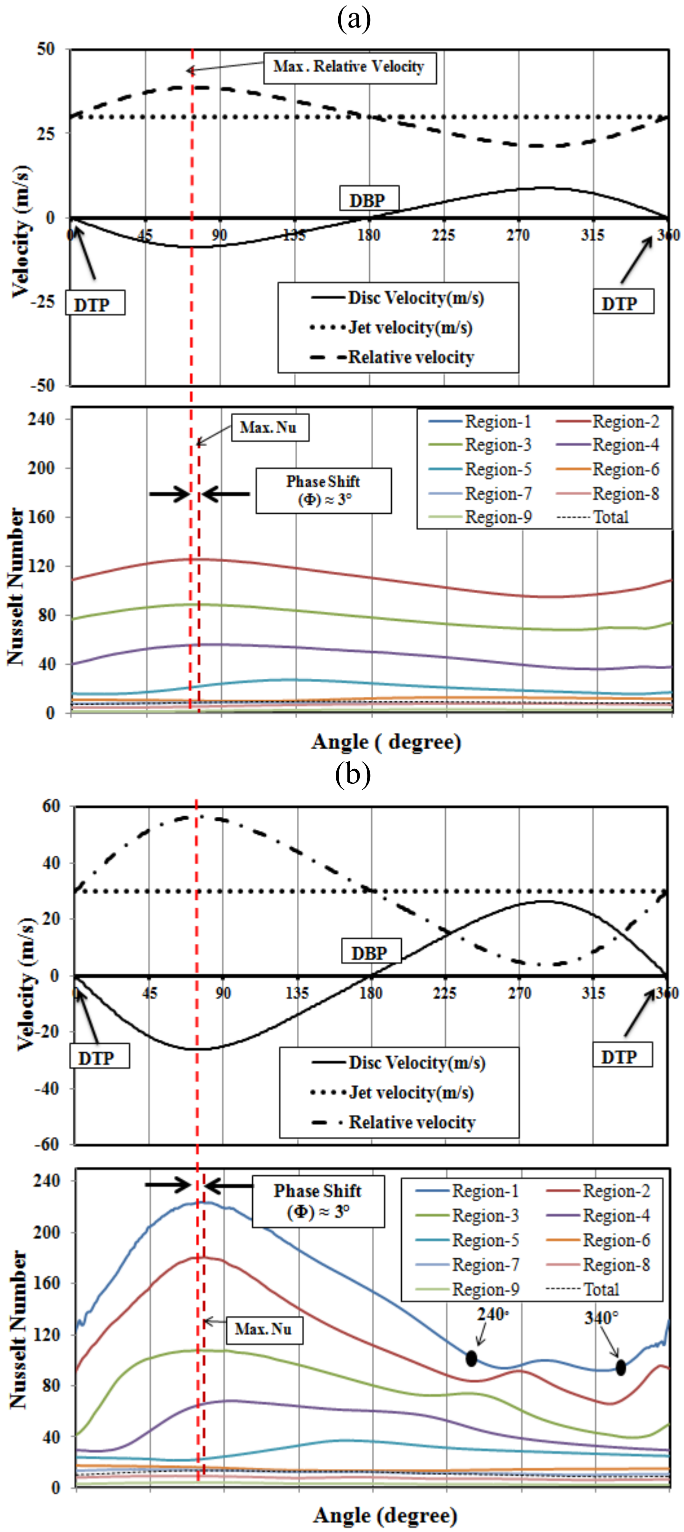

Figure 6 Steady state profiles of Nusselt number for moving disc with cooling jet: (a) ω = 210 rad/s, (b) ω = 630 rad/s

The reason that the Nusselt number profile lags behind the maximum relative velocity can be attributed to the phase shift between the occurrence of maximum radial velocity in the vicinity of the impinging surface and maximum relative velocity between the jet and moving disc. More insight into this observation can be gained by examining the evolution of maximum radial velocity in the vicinity of the impinging zone for the angular velocity 630 rad/s, as shown in Figure 7. The upper-right corner in this figure is the stagnation point, the wall jet flows radially from stagnation point to the left. As shown in this figure and the data recorded to the right, the maximum relative velocity occurs at Θ = 75°, while the maximum radial velocity associated with maximum Nusselt number occurs at Θ = 77°- 78°.

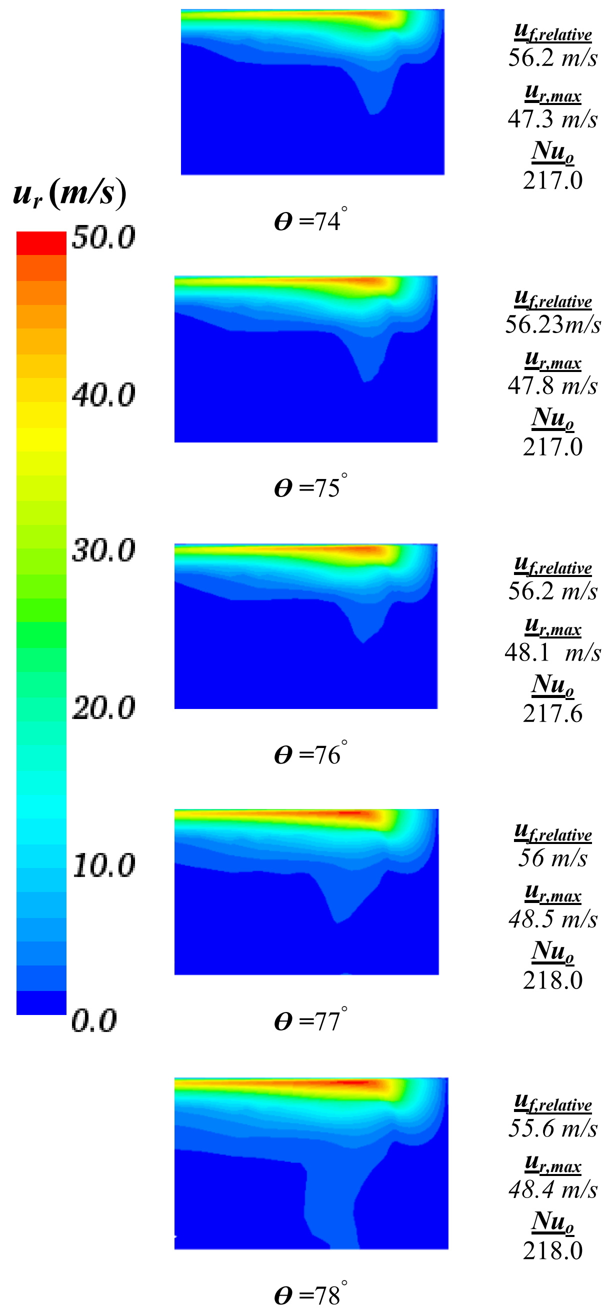

Figure 7 Evolution of maximum radial velocity in the vicinity of the impingement surface (ω = 630 rad/s)

The temperature profiles in the disc for both angular velocities are shown in Figure 8. The heat transfer coefficients and corresponding Nusselt numbers averaged over one cycle for the first four regions at the fluid-solid interface (shown in Figure 3) are given in Table 2. A close examination of Figure 8 and Table 2 reveals that the volume average temperature and stagnation zone temperature are less with angular velocity 630 rad/s. Although the relative velocity between the jet and moving disc is close to the zero for some period of time during the cycle in this case, the cooling effect is more efficient compared with the angular velocity 210 rad/s, because the higher relative velocity between the disc and jet (during the rest of the cycle) compensates for the lack in heat transfer coefficient and enhances the cooling efficiency. A comparison between the stagnation zone temperature for both the moving and stationary discs reveals a reduction of 1.5% with the moving boundary. Increasing the jet velocity will increase the relative velocity in case of a moving boundary and hence decrease the stagnation zone temperature.

The surface average temperature of the entire interface and the first four regions at the fluid-solid interface for all cases considered in the current study is summarized in Table 3.

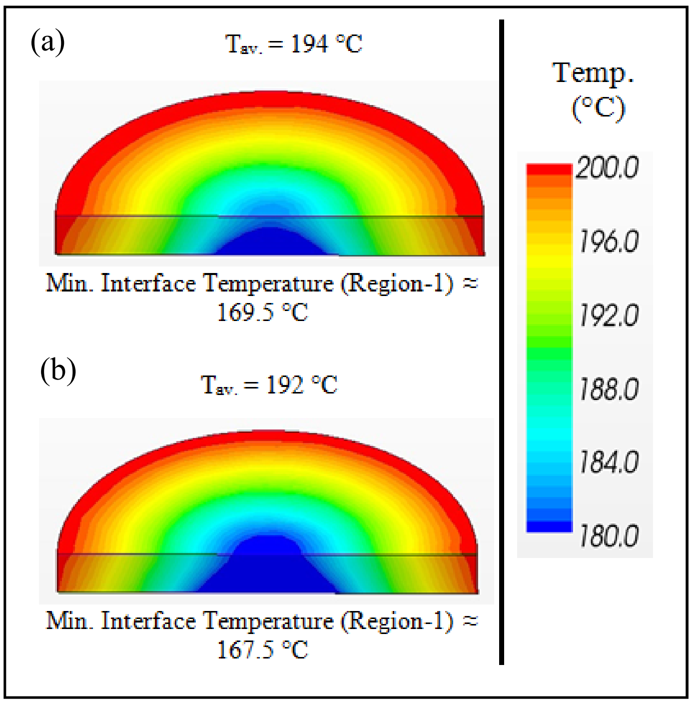

Figure 8 Steady state temperature profile for moving disc with cooling jet: (a) ω = 210 rad/s, (b) ω = 630 rad/s

Region No.	*Nu*	*HTC ($W/m^2.K$)*
Region-1	146	19554
Region-2	109	14645
Region-3	77	10332
Region-4	46	6171
Total Surface Av.	**9**	**1184**

Region No.	*Nu*	*HTC ($W/m^2.K$)*
Region-1	149	19908
Region-2	116	15560
Region-3	77	10279
Region-4	49	6531
Total Surface Av.	**11**	**1523**

Table 2 Surface average Nusselt number at solid-fluid interface with cooling jet: (a) ω = 210 rad/s, (b) ω= 630 rad/s

Boundary	Cooling	R-1	R-2	R-3	R-4	Interface Av.
Stationary	Jet-20 mm *Re* ≈ 3000	172°	173.5°	176°	179.5°	194.5°
Stationary	Jet-100 mm *Re* ≈ 3000	170.5°	171.5°	174°	177°C	192°
Moving 210 rad/s	No jet	210°	210°	210°	210°	205°
Moving 630 rad/s	No jet	210°	209.5°	209.5°	209.5°	205°
Moving 210 rad/s	Jet *Re* ≈ 3000	169.5°	170.5°	173°	177°	192.5°
Moving 630 rad/s	Jet *Re* ≈ 3000	167.5°	168.5°	171°	174.5°	190.5°

Table 3 Surface average of steady state temperature for regions illustrated in Figure 3

CONCLUSION

Numerical studies of a circular oil jet impinging on both stationary and moving (reciprocating) discs subjected to uniform wall heat flux were carried out using the volume of fluid (VOF) method. The conclusions can be summarized as follow:

- For stationary boundary, the stagnation zone and disc volume average temperatures are smaller for longer jets in comparison with shorter jets. It appears that the dynamics of the interaction is different with more splattering occurring in the shorter jet.
- Although the relative velocity between the jet and moving disc is close to zero for some time during the cycle in the case of the higher angular velocity, the cooling effect is more efficient than the lower angular velocity. The higher relative velocity between the disc and jet (during the rest of the cycle) compensates for the lack in heat transfer coefficient and enhances the cooling efficiency.
- For jet impingement onto a moving boundary, the maximum Nusselt number is achieved a short time after the relative velocity between the disc and the jet reaches its maximum. The jet turning process at the stagnation zone, which aligns the jet parallel to the target surface, will lag the occurrence of the maximum HTC by a few degrees.

REFERENCES

[1] Liu, X., Lienhard, J.H., and Lombara, S., 1991, "Convective Heat Transfer by Impingement of Circular Liquid Jets", J. Heat Transfer, Vol. 113(3), pp. 571-582.

[2] Ichimiya, K., Takema, S., Morimoto, S., Kunugi, T., and Akino, N., 2001, "Movement of Impingement Heat Transfer by a Single Circular Jet with a Confined Wall", Int. J. Heat and Mass Transfer, Vol. 44, pp. 3095-3102.

[3] Ashforth, S., Jambunathan, K., and Whitney, C.F., 1997, "Velocity and Turbulence Characteristics of Semiconfined Orthogonally Impinging Slot Jet", Experimental Thermal and Fluid Science, Vol. 14, pp. 60-67.

[4] Liu, X., Gabour, L.A., and Lienhard, J.H., 1993, "Stagnation-Point Heat Transfer During Impinging of Laminar Liquid Jets: Analysis Including Surface Tension", J. Heat Transfer, Vol. 115, pp. 99-105.

[5] Liu, X., and Lienhard, J.H., 1989, "Liquid Jet Impingement Heat Transfer on a Uniform Flux Surface", ASME Heat Transfer Division, Book No. H00498, Vol. 106, pp. 523-530.

[6] Agarwal, A.K., Goyal, S.K., and Srivastava, D.K., 2011, "Time Resolved Numerical Modelling of Oil Jet Cooling of a Medium Duty Diesel Engine Piston", International Communications in Heat and Mass Transfer, Vol. 38, pp. 1080-1085.

[7] Hewakandamby, B.N., 2009, "A Numerical Study of Heat Transfer Performance of Oscillatory Impinging Jets," Int. J. Heat and Mass Transfer, Vol. 52, pp. 396- 406.

[8] Xu, F., and Gadala, M.S., 2006, "Heat Transfer Behaviour in the Impingement Zone under Circular Water Jet", Int. J. Heat and Mass Transfer, Vol. 49, pp. 3785-3799.

[9] Rahman, M.M., Bula, A.J., and Leland, J., 1999, "Conjugate Heat Transfer during Free Jet Impingement of a High Prandtl Number Fluid", Numerical Heat Transfer, Part B, Vol. 36, pp. 139-162.

[10] Nasif, G., Barron, R.M., Balachandar, R., and Iqbal, O., 2013, "Simulation of Jet Impingement Heat Transfer", ASME 2013 Internal Combustion Engine Division (ICED), Fall Technical Conference, Dearborn, MI.

[11] Lienhard, J.H., 2006, "Heat Transfer by Impingement of Circular Free-Surface Liquid Jets", 18th National and 7th ISHMT-ASME, Heat and Mass Transfer Conference, Guwahati, India.

[12] Nasif, G., Barron, R.M., and Balachandar, R., 2013, "Jet Impingement Heat Transfer", International Conference on Advancements and Futuristic Trends in Mechanical and Materials Engineering, Kapurthala, Punjab, India

[13] Stevens, J., and Webb, B.W., 1991, "Local Heat Transfer Coefficients under an Axisymmetric, Single Phase Liquid Jet", J. Heat Transfer, Vol. 113(1), pp. 71-78.

[14] Muzaferija, S., Peric, M., Sames, P., and Schelin, T., 1998, "A Two-Fluid Navier-Stokes Solver to Simulate Water Entry", Proceedings Twenty-Second Symposium on Naval Hydrodynamics, Washington, D.C., USA, pp. 638-651.